GEOPHYSICAL RESEARCH LETTERS, VOL. 35, L23205, doi:10.1029/2008GL035620, 2008

Volcanism on Mercury: A new model for the history of magma ascent and eruption

Lionel Wilson[1,2] and James W. Head[2]

Received 7 August 2008; revised 15 October 2008; accepted 17 October 2008; published 6 December 2008.

[1] We use the identification of volcanism on Mercury, together with lobate, flow-front like topography, crustal composition information and data on the stress state and history of the lithosphere, to derive a new model for the ascent and eruption of magma on Mercury. We find that extrusion is likely to be dominated by high-effusion rate events. Initial emplacement of dikes in the crust and extrusions to the surface will result in a denser crust, favoring even more extrusive volcanism. This will be followed by cooling associated with planetary thermal evolution that will rapidly decrease the ability of magma to reach the surface, resulting in a decline and termination of volcanism following the emplacement and deformation of regional smooth plains. These predictions and the resulting history can be tested with observations from missions to Mercury. **Citation:** Wilson, L., and J. W. Head (2008), Volcanism on Mercury: A new model for the history of magma ascent and eruption, *Geophys. Res. Lett.*, *35*, L23205, doi:10.1029/2008GL035620.

1. Introduction

[2] Volcanism on one-plate planets [*Solomon*, 1978] commonly involves buoyant rise of mantle diapirs and mantle partial melting. Magma reaches the surface through dike propagation in the brittle part of the crust/lithosphere, ending in extrusion to the surface and the formation of vents, edifices and plains deposits. The ease with which magma reaches the surface is directly related to the density of the crust (low-density crusts can form magmatic density traps and inhibit ascent and eruption of magma), and the global state of stress in the lithosphere (net extensional deformation enhances the ability of dikes to propagate to the surface, but a net contractional state of stress inhibits magma ascent and eruption) [*Solomon*, 1977a, 1978; *Head and Wilson*, 1992]. On the Moon, the global state of stress changed from net extension to net contraction during the period of mare volcanism, coincident with overall lunar thermal evolution and the thickening of the lithosphere [*Solomon*, 1977b; *Solomon and Head*, 1980]. The flux of lunar volcanism decreased drastically in the period following this change [e.g., *Head and Wilson*, 1992; *Hiesinger et al.*, 2000].

[3] On Mercury, the paucity of graben and the dominance of ridges and huge scarps interpreted to be of contractional origin strongly suggest that the net state of stress in the lithosphere has been contractional during much of its history [*Strom et al.*, 1975; *Melosh and McKinnon*, 1988], and therefore that dike propagation might be much more inhibited, and volcanism much less extensive, than on the Moon. Indeed, Mariner 10 observations, while revealing extensive regional plains, failed to resolve the debate between their volcanic origin [*Murray et al.*, 1975; *Strom et al.*, 1975; *Robinson and Lucey*, 1997] or an origin as ponded impact ejecta [*Wilhelms*, 1976]. Recent MESSENGER data provide evidence that extensive areas of smooth plains on Mercury are volcanic [*Head et al.*, 2008; *Robinson et al.*, 2008; *Murchie et al.*, 2008], helping to resolve this decades-old debate. The new MESSENGER data also show that the total contractional strain is at least one-third greater than that estimated from Mariner 10 images, and also confirms Earth-based observations that the crust is low in Fe [*Solomon et al.*, 2008]. These developments provide reasons to reexamine the morphology of plains on Mercury and to undertake a new assessment of eruption conditions that might explain the characteristics of volcanic plains. Here we develop a new approach that combines 1) interpretation of lobate flow-like fronts to assess likely effusion rates, 2) density models that provide information on plausible dike widths and implied modes of emplacement, and 3) the state and magnitude of stress in the lithosphere.

2. Interior Structure and Thermal Evolution

[4] There is great uncertainty about the details of the structure and composition of the crust, mantle and core of Mercury [e.g., *Hauck et al.*, 2004]. For example, the high mean density of the body suggests that it may have lost parts of its crust and mantle in a giant impact [e.g., *Cameron et al.*, 1988] at some stage after most of its initial accretion was sufficiently complete that at least partial separation of a core had occurred. It is this type of uncertainty about the physico-chemical state of proto-Mercury that leads to difficulties in predicting the structure of the crust and mantle. However, it is reasonable to assume that the Mercury we see today has some combination of a relatively low-density crust and a relatively high-density mantle [*Hauck et al.*, 2004].

[5] The presence of planet-wide systems of wrinkle ridges and thrust faults on Mercury implies that a compressive crustal stress regime became dominant relatively early in the history of Mercury [*Strom et al.*, 1975]. The fact that these folds and faults produced by the compressive regime deform many stratigraphically young plains units [*Spudis and Guest*, 1988] suggests that the development of the compressive stresses may have played a vital role in determining when and if surface eruptions of mantle-derived magmas could occur. This would be analogous to the way in which the change with time from extensional to compressive global stresses in the lithosphere of the Moon

[1]Environmental Science Department, Lancaster University, Lancaster, UK.
[2]Geological Sciences Department, Brown University, Providence, Rhode Island, USA.

0094-8276/08/2008GL035620$05.00

Table 1. Minimum Depths of Melt Sources, H_m, Allowing Surface Eruptions, as a Function of Crustal Thickness, H_c[a]

	Crustal Density 2600			Crustal Density 2700			Crustal Density 2800		
H_c/km	H_m/km	S_u/MPa	S_v/MPa	H_m/km	S_u/MPa	S_v/MPa	H_m/km	S_u/MPa	S_v/MPa
20	40	11	22	35	8	17	30	5.5	10
30	60	22	33	52	13	23	45	8.3	19
40	80	33	44	70	23	33	60	11	22
50	100	44	56	88	32	43	75	17	28
60	120	56	67	105	40	49	90	22	35
70	140	67	78	122	46	57	105	28	39

[a]Also given are the maximum horizontal compressive stresses allowed if a dike is to remain open at all depths, S_u when the stress is uniform with depth in the crust and S_v when the stress decreases with depth. These values are given for a mantle density, 3400 kg m^{-3}; a melt density, 3000 kg m^{-3}; and for three crustal densities, 2600, 2700 and 2800 kg m^{-3}.

influenced the viability of erupting magmas from deep mantle sources [*Solomon and Head*, 1980; *Head and Wilson*, 1992].

3. Analysis

[6] To investigate the relationship between lithospheric stresses and magma eruption conditions [e.g., *Head and Wilson*, 1992; *Wilson and Head*, 2008] we have assumed a series of permutations of crustal density, ρ_c, crustal thickness, H_c, mantle density, ρ_m, magma density, ρ_v, source depth below the surface of mantle melt being erupted, H_m, and crustal compressive stress, S, and investigated which permutations will allow the transfer of magma from source to surface. The key issues are that to provide a significant quantity of magma for a prolonged eruption (i) the lithostatic pressure at the magma source depth must be able to support a column of magma at least as far as the surface (any excess pressure is available to drive the magma motion against friction with the walls of the dike), and (ii) the stress gradient across the walls of the dike acting to close it must not exceed the stress gradient due to the internal pressure distribution acting to keep it open [e.g., *Rubin and Pollard*, 1987; *Wilson and Head*, 2002]. Condition (i) is just satisfied if $H_c\rho_c + (H_m - H_c)\rho_m = H_m\rho_v$, so the minimum magma source depth is given by

$$H_m = H_c[(\rho_m - \rho_c)/(\rho_m - \rho_v)] \quad (1)$$

Condition (ii) is not easy to define analytically but corresponds to equating the compressive stress S to the dike driving pressure, defined as the maximum value of the difference between the magma pressure inside the dike and the total external closure stress (i.e., lithostatic load plus S).

[7] Given the large number of variables it is easiest to illustrate the results by choosing one set of densities and varying the depths and stresses. We first adopt ρ_c = 2600 kg m^{-3}, ρ_m = 3400 kg m^{-3} and ρ_v = 3000 kg m^{-3}. Table 1 then shows, as a function of the thickness of the crust (H_c), the minimum depth below the surface (H_m) from which mantle melts must be derived if their positive buoyancy in the mantle is to just compensate for their negative buoyancy in the crust and so enable them to reach the surface and erupt. For the values of H_m in Table 1 to be valid, the stress conditions in the crust must be such that a dike can remain open at all depths. However, this may not be possible in the presence of a horizontal compressive stress. The third and fourth columns of Table 1 show the maximum horizontal compressive stress allowed if a dike is to remain open when the compressive stress is either uniform, i.e., the same at all depths in the crust (S_u), or variable, specifically decreasing linearly from the value given (S_v) at the surface to zero at the base of the crust to simulate the progressive change in host rock rheology from elastic to plastic.

[8] We now increase the crustal density slightly to 2700 kg m^{-3} but keep the mantle and melt densities the same. The results show, as expected, that the reduced amount of negative buoyancy of magma in the crust means that mantle melt sources need not be quite as deep as before. However, if a pathway is to remain open at all depths, significantly smaller compressive stresses must be present than in the previous case. This trend continues as crustal density increases further to 2800 kg m^{-3}. In view of the MESSENGER finding that contractional strain is greater than estimated from Mariner 10 data [*Solomon et al.*, 2008], this suggests that a relatively low crustal density, consistent with the low Fe content of the crust, may have been an important factor in allowing eruptive activity to occur.

4. Lobate Flow Fronts and Implications

[9] A series of lobate flow fronts have been mapped on Mercury and these provide part of the evidence for the volcanic origin of smooth plains [e.g., *Spudis and Guest*, 1988]. These features (Figure 1) provide important information about candidate eruption conditions. Photoclinometry [e.g., *Mouginis-Mark and Wilson*, 1981] was used to measure topographic profiles across some of the smooth plains unit margins arrowed in Figure 1, assuming that at a constant phase angle (i.e., within a single image) the surface reflects light in proportion to the Lommel-Seeliger function [$\cos \iota/(\cos \iota + \cos \varepsilon)$] where ι and ε are the angles from the surface normal of the incident and scattered light, respectively. It is clear from evaluating mean surface brightness values on either side of unit boundaries that the plains units are about 10% less reflective than the terrains they embay, and the chief uncertainty in the analysis is the way in which the albedo changes in crossing from one unit to another. Figure 2 shows the profiles generated for an embayment contact near the middle of Figure 1a as the location of the albedo change is moved across the boundary. The profiles cannot be interpreted unambiguously: the boundary could define either the 180 m high edge of a lava flow with an interior that has drained by an amount that could lie between ~160 m and ~60 m (profiles 1 through 7) or a large wrinkle ridge marking an elevation offset of ~20 m to ~120 m that may be caused by a thrust fault. Without stereoscopy or laser altimetry these options are all possible. However, the fact that the plains unit is ~10% less reflective than the terrain it embays lends support to the idea that it is

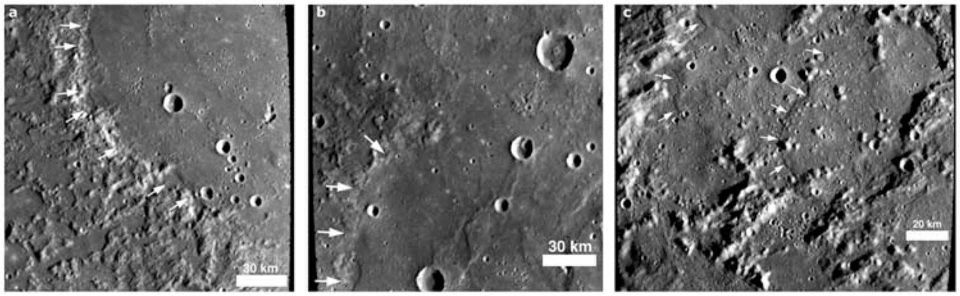

Figure 1. Smooth plains on Mercury; arrows show lobes: (a) embaying the margin of Van Eyck; (b) embaying the Odin Formation. (c) Lobes within the Nervo Formation. Modified from *Milkovich et al.* [2002]. North is at the top in each case. Figure 2 profile is located between third and fourth arrow from the top in Figure 1a.

compositionally different or has experienced a different history of space weathering and hence differs in age. Interpreting the boundary as a lava flow margin means that the flow margin thickness must be ~180 m.

[10] The thicknesses, T, of the interpreted lava flow margins can be related to the lava yield strengths, Y, if the local slope, α, is known. Equating the basal shear stress to the yield strength,

$$Y = (T\rho g \sin\alpha) \tag{2}$$

where g is the acceleration due to gravity, 2.78 m s^{-2}, and we assume a lava density of ρ = 2000 kg m^{-3} which corresponds to ~30% vesicularity in a mafic lava of density ~2800 kg m^{-3}. *Kreslavsky et al.* [2008] give the average variation of α with horizontal scale length for Mercury, and at the scale lengths of 10s of km relevant here, α = ~0.3°. Using this value, a margin height of ~180 m implies a yield strength of ~5300 Pa. Given the range of lava densities and vesicularities found on Earth, ρ is not likely to be less than 1000 or more than 3000 kg m^{-3} and *Kreslavsky et al.*'s [2008] analysis implies that α is almost certainly more than 0.2°. Thus this yield strength estimate is unlikely to be uncertain by more than a factor of ~2. While there is no unique relationship between yield strength and composition for lavas, this value is entirely typical of mafic lavas on Earth (e.g., see summary by *Wilson and Head* [1994]).

[11] The possibility that these flows have redistributed lava by drainage suggests that their interiors were relatively hot immediately after their emplacement. This is consistent with the rapid emplacement of lava over wide areas from high effusion rate eruptions, and with the paucity of observed vents, since such flows are the most likely to drown their vents, a process that seems to have been common on the Moon [*Head and Wilson*, 1992]. A minimum estimate of eruption rate can be obtained by assuming that flows are cooling-limited [*Pinkerton and Wilson*, 1994], in which case the volume effusion rate V and observed flow length L are related by

$$V = (L\kappa Gzw)/(\beta T) \tag{3}$$

where w and T are the width and thickness of the flow, κ is the thermal diffusivity of the lava (generally close to 7 × 10^{-7} m^2 s^{-1}), Gz is a critical value of the dimensionless Grätz number, and β is a factor that depends on the ratio of the effective hydraulic radius of the flow to its actual depth. Observed values of Gz are found to lie in the range 280 to 370 with an average close to 300 [*Pinkerton and Wilson*, 1994]. For flows that are coming to rest due to cooling, the cooled surface crust will not be moving as fast as the hotter lava in the core of the flow and the relevant value of β is 4. Observations of putative flow fields on Mercury (Figure 1) suggest we take L to be at least ~100 km and w to be at least ~30 km; then with T = ~120 m we find V = ~1–2 × 10^3 m^3 s^{-1}. This value is comparable to the largest historic eruption rates observed in basaltic fissure eruptions on Earth (summarized by *Wilson and Head* [1981]) and about a factor of 3 less than the eruption rates required to generate the source depressions of thermally eroded sinuous rilles on the Moon [*Head and Wilson*, 1981] and Mars [*Wilson and Head*, 1994]. We note that no sinuous rille channels have yet been identified on Mercury [*Milkovich et al.*, 2002] in Mariner 10 or MESSENGER data.

[12] Finally we note that typical flow speeds, u, can be estimated for these lavas. If the flow motion is laminar, the speed is given by

$$u = \left(\rho g T^2 \sin\alpha\right)/(3\eta) \tag{4}$$

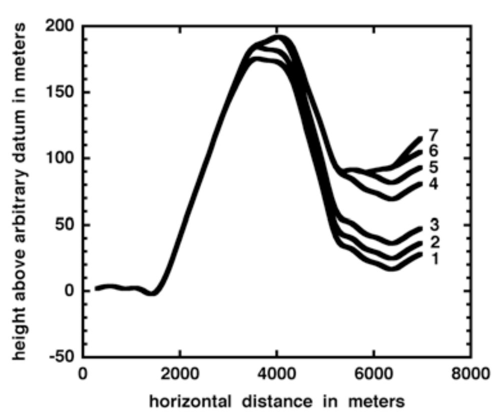

Figure 2. Topographic profile across the western smooth plains unit boundary between third and fourth arrow from the top in Figure 1a. The profiles differ only in the selection of the location of the boundary where the albedo changes: the change occurs 2900, 3480, 4060,5220, 5800, 6380 and 6960 m from the left edges of profiles 1 through 7, respectively.

where η is the lava viscosity, and for turbulent motion the equivalent is

$$u = [(2gT \sin \alpha)/K]^{1/2} \tag{5}$$

where K is a friction factor with a value of $\sim$0.01 [*Wilson and Head*, 1981]. With T = $\sim$180 m and α = $\sim$0.3°, equation (5) implies u = $\sim$24 m s^{-1}. We do not know the viscosity of lavas on Mercury, but if we adopt a wide range for mafic lavas, say 1 to 1000 Pa s, equation (4) would predict laminar low speeds in the range $\sim$200 to $\sim$200,000 m/s. These would correspond to Reynolds numbers, Re = $(2T\rho u)/\eta$, in the range 10^5 to 10^{11}, all grossly inconsistent with laminar flow which requires Re less than $\sim$2000. Only if the lava viscosity were greater than 10,000 Pa s, a value appropriate to an andesitic composition on Earth [*McBirney and Murase*, 1984], would the laminar formula become relevant and start to predict flow speeds less than $\sim$24 m s^{-1}. Thus unless they have viscosities of this order, flows $\sim$180 m thick on Mercury, even on the shallow slopes inferred here, would be emplaced under turbulent conditions at speeds of $\sim$24 m s^{-1}. Travel distances of $\sim$100 km would then imply emplacement times of $\sim$4200 s, i.e., $\sim$1 hour. Also, flow dimensions of $\sim$100 km $\times$ 30 km $\times$ 120 m correspond to a volume of $\sim$360 km^3, and emplacement of this volume in $\sim$4200 s would imply a volume eruption rate of $\sim 8 \times 10^7$ m^3 s^{-1}. This is more than four orders of magnitude greater than the cooling-limited eruption rate deduced above, and would imply that flows were volume-limited rather than cooling-limited. Reality presumably lies between these extremes. Given the ratio of the accelerations due to gravity, a flow thickness of $\sim$180 m on Mercury corresponds to a thickness of $\sim$50 m on Earth for the same lava yield strength. Flood-basalt flow units with thicknesses of this order on Earth are widely assumed to have reached their maximum extents as thinner flows under cooling-limited conditions and to then have inflated as the magma supply continued [*Thordarson and Self*, 1998]. A similar process may occur on Mercury, with both inflation in places and subsequent deflation of some flow lobe interiors as lava is redistributed into new lobes growing elsewhere in the same compound flow field.

5. Discussion and Conclusions

[13] On the basis of lobate flow front heights, coupled with the lateral extents of these flow units, we infer that they could readily be understood as the products of high-effusion rate, large-volume eruptions of mafic lava analogous to flood-basalts on Earth. This would also help explain the paucity of vents and constructional edifices.

[14] Our analysis of the ability of magma to reach the surface on Mercury has shown that a high crustal density makes it easier, in terms of magma buoyancy alone, to erupt magma from a given depth in the mantle. Given that all intrusions and eruptions emplace magma at some level into the crust, and therefore increase its density with time, this at first sight implies that surface eruptions of magma coming directly from the mantle could have become more common with time on Mercury. However, the thermal history of the planet is likely to dictate that crustal compressive stresses increased with time [*Solomon*, 1977a, 1978; *Hauck et al.*, 2004]. We have found that such an increase progressively suppresses the possibility of maintaining continuously open pathways between the mantle and the surface, but that this trend can be counteracted by a low crustal density. Taken together, these results suggest that conditions allowing eruptions to occur were very finely balanced. By analogy with the Moon's thermal history [*Wieczorek et al.*, 2007], compressive stresses at least a factor of two greater than those found here to be able to suppress stable dikes must have been reached part way through Mercury's lifetime, with even greater compressive stresses being needed to cause the observed thrust faults [*Strom et al.*, 1975; *Melosh and McKinnon*, 1988; *Solomon et al.*, 2008]. This would have caused deep-seated eruptive activity to have ceased on Mercury, with the timing of the cessation being very finely tuned by the planet's density and stress structure. As our knowledge of internal structure, crustal composition, flow unit topography and ages, and temporal relations to scarp formation improves, it will become possible to greatly refine these initial models.

References

Cameron, A. G. W., B. Fegley Jr., W. Benz, and W. L. Slattery (1988), The strange density of Mercury: Theoretical considerations, in *Mercury*, edited by F. Vilas, C. R. Chapman, and M. S. Matthews, pp. 692–708, Univ. of Arizona Press, Tucson.

Hauck, S. A., A. J. Dombard, R. J. Phillips, and S. C. Solomon (2004), Internal and tectonic evolution of Mercury, *Earth Planet. Sci. Lett.*, *222*, 713–728.

Head, J. W., and L. Wilson (1981), Lunar sinuous rille formation by thermal erosion: Eruption conditions, rates and durations, *Lunar Planet. Sci.*, 427–429.

Head, J. W., and L. Wilson (1992), Lunar mare volcanism: Stratigraphy, eruption conditions, and the evolution of secondary crusts, *Geochim. Cosmochim. Acta*, *55*, 2155–2175.

Head, J. W., et al. (2008), Volcanism on Mercury: Evidence from the first MESSENGER flyby, *Science*, *321*, 69–72.

Hiesinger, H., R. Jaumann, G. Neukum, and J. W. Head (2000), Age of mare basalts on the lunar nearside, *J. Geophys. Res.*, *105*, 29,239–29,275.

Kreslavsky, M. A., J. W. Head, and J. K. Harmon (2008), Large-scale topographic roughness of terrestrial planets: A comparison, *Lunar Planet. Sci.*, *XXXIX*, Abstract 1472.

McBirney, A. R., and T. Murase (1984), Rheological properties of magmas, *Annu. Rev. Earth Planet. Sci.*, *12*, 337–357.

Melosh, H. J., and W. B. McKinnon (1988), The tectonics of Mercury, in *Mercury*, edited by F. Vilas, C. R. Chapman, and M. S. Matthews, pp. 401–428, Univ. of Arizona Press, Tucson.

Milkovich, S. M., J. W. Head, and L. Wilson (2002), Identification of Mercurian volcanism: Resolution effects and implications for MESSENGER, *Meteorol. Planet. Sci.*, *37*, 1209–1222.

Mouginis-Mark, P. J., and L. Wilson (1981), MERC: A FORTRAN IV program for the production of topographic data for the planet Mercury, *Comput. Geosci.*, *7*, 35–45.

Murchie, S. L., et al. (2008), Geology of the Caloris basin, Mercury: A view from MESSENGER, *Science*, *321*, 73–76.

Murray, B. C., R. G. Strom, N. J. Trask, and D. E. Gault (1975), Surface history of Mercury: Implications for terrestrial planets, *J. Geophys. Res.*, *80*, 2508–2514.

Pinkerton, H., and L. Wilson (1994), Factors controlling the lengths of channel-fed lava flows, *Bull. Volcanol.*, *56*, 108–120.

Robinson, M. S., and P. G. Lucey (1997), Recalibrated Mariner 10 color mosaics: Implications for Mercurian volcanism, *Science*, *275*, doi:10.1126/science.275.5297.197.

Robinson, M. A., et al. (2008), Reflectance and color variations on Mercury: Indicators of regolith processes and compositional heterogeneity, *Science*, *321*, 66–69.

Rubin, A. M., and D. D. Pollard (1987), Origins of blade-like dikes in volcanic rift zones, in *Volcanism in Hawaii*, edited by R. W. Decker, T. L. Wright, and P. M. Stauffer, *U.S. Geol. Surv. Prof. Pap.*, *1350*, 1149–1470.

Solomon, S. C. (1977a), The relationship between crustal tectonics and internal evolution in the Moon and Mercury, *Phys. Earth Planet. Inter.*, *15*, 135–145.

Solomon, S. C. (1977b), Mare volcanism and lunar crustal structure, *Proc. Lunar Sci. Conf.*, *6th*, 1021–1042.

Solomon, S. C. (1978), On volcanism and thermal tectonics on one-plate planets, *Geophys. Res. Lett.*, *5*, 461–464.

Solomon, S. C., and J. W. Head (1980), Lunar mascon basins: Lava filling, tectonics and evolution of the lithosphere, *Rev. Geophys.*, *18*, 107–141.

Solomon, S. C., et al. (2008), Return to Mercury: A global perspective on MESSENGER's first Mercury flyby, *Science*, *321*, 59–62.

Spudis, P. D., and J. E. Guest (1988), Stratigraphy and geological history of Mercury, in *Mercury*, edited by F. Vilas, C. R. Chapman, and M. S. Matthews, pp. 118–164, Univ. of Arizona Press, Tucson.

Strom, R., N. Trask, and J. Guest (1975), Tectonism and volcanism on Mercury, *J. Geophys. Res.*, *80*, 2478–2507.

Thordarson, T., and S. Self (1998), The Roza Member, Columbia River Basalt Group: A gigantic pahoehoe lava flow field formed by endogenous processes?, *J. Geophys. Res.*, *103*, 27,411–27,445.

Wieczorek, M. A., et al. (2007), The constitution and structure of the lunar interior, in *New Views of the Moon*, *Mineral. Soc. Am. Rev. Mineral. Geochem.*, *60*, 221–364.

Wilhelms, D. (1976), Mercurian volcanism questioned, *Icarus*, *28*, 551–558.

Wilson, L., and J. W. Head (1981), Ascent and eruption of basaltic magma on the Earth and Moon, *J. Geophys. Res.*, *86*, 2971–3001.

Wilson, L., and J. W. Head (1994), Mars: Review and analysis of volcanic eruption theory and relationships to observed landforms, *Rev. Geophys.*, *32*, 221–263.

Wilson, L., and J. W. Head III (2002), Tharsis-radial graben systems as the surface manifestation of plume-related dike intrusion complexes: Models and implications, *J. Geophys. Res.*, *107*(E8), 5057, doi:10.1029/2001JE001593.

Wilson, L., and J. W. Head (2008), Eruption rates of mare lava flows on the Moon and implications for mantle melt volumes and dike geometries, *Lunar Planet. Sci.*, *XXXIX*, Abstract 1104.

J. W. Head, Geological Sciences Department, Brown University, Box 1846, Providence, RI 02912, USA. (james_head_III@brown.edu)

L. Wilson, Environmental Science Department, Lancaster University, Lancaster LA1 4YQ, UK.